AD-A090 496 COLLEGE OF WILLIAM AND MARY WILLIAMSBURG VA DEPT OF --ETC F/G 7/2
A STUDY OF THE COLLISIONAL DYNAMICS FOR COLLISIONS OF UF6(-) WI--ETC(U)
AUG 80 L D DOVERSPIKE, R L CHAMPION F49620-79-C-0219
UNCLASSIFIED U3 AFOSR-TR-80-1062 NL

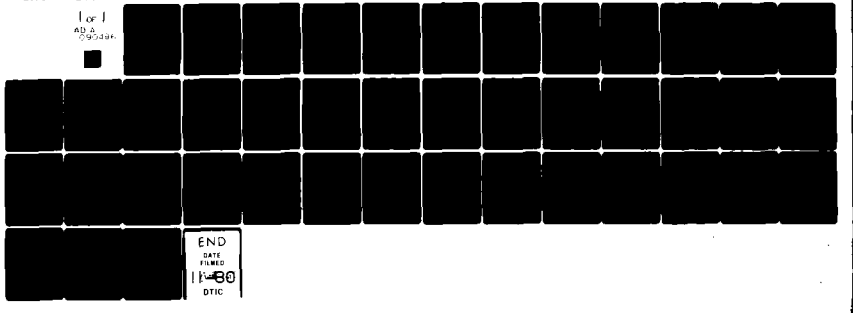

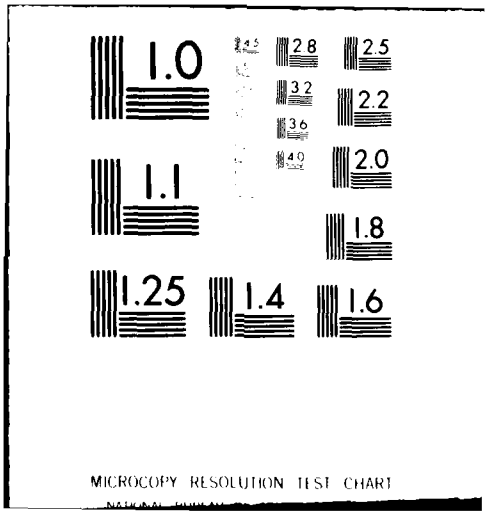
1.0
2.8
2.5
3.2
2.2
3.6
4.0
2.0
1.1
1.8
1.25
1.4
1.6
MICROCOPY RESOLUTION TEST CHART

Report U3

FINAL SCIENTIFIC REPORT

for

AFOSR CONTRACT F49620-79-C-0219

LEVEL II

"A Study of the Collisional Dynamics for Collisions of UF_6 with Atoms and Molecules"

by

L. D. Doverspike

and

R. L. Champion

Department of Physics

College of William and Mary

Williamsburg, Virginia 23185

August 1980

AIR FORCE OFFICE OF SCIENTIFIC RESEARCH (AFSC)
NOTICE OF TRANSMITTAL TO DDC
This technical report has been reviewed and is
approved for public release IAW AFR 190-12 (7b).
Distribution is unlimited.
A. D. BLOSE
Technical Information Officer

SECURITY CLASSIFICATION OF THIS PAGE (When Data Entered) UNCLASSIFIED

A. REPORT DOCUMENTATION PAGE	READ INSTRUCTIONS BEFORE COMPLETING FORM
1. REPORT NUMBER: AFOSR-TR-80-1062	2. GOVT ACCESSION NO.: AD-A090496 ✓
	3. RECIPIENT'S CATALOG NUMBER:
4. TITLE (and Subtitle): A Study of the Collisional Dynamics for Collisions of UF_6^- with Atoms and Molecules	5. TYPE OF REPORT & PERIOD COVERED: Final; 1 July 1979-30 June 80
	6. PERFORMING ORG. REPORT NUMBER:
7. AUTHOR(s): L. D. Doverspike and R. L. Champion	8. CONTRACT OR GRANT NUMBER(s): F49620-79-C-0219
9. PERFORMING ORGANIZATION NAME AND ADDRESS: College of William and Mary, Department of Physics ✓, Williamsburg, Virginia 23185	10. PROGRAM ELEMENT, PROJECT, TASK AREA & WORK UNIT NUMBERS: 61102F, 2301/A5
11. CONTROLLING OFFICE NAME AND ADDRESS: Air Force Office of Scientific Research/NP, Directorate of Physics, Bolling AFB, D. C. 20332	12. REPORT DATE: August 1980
	13. NUMBER OF PAGES: 42
14. MONITORING AGENCY NAME & ADDRESS (if different from Controlling Office)	15. SECURITY CLASS. (of this report): UNCLASSIFIED
	15a. DECLASSIFICATION/DOWNGRADING SCHEDULE

16. DISTRIBUTION STATEMENT (of this Report)

Approved for public release; distribution unlimited.

17. DISTRIBUTION STATEMENT (of the abstract entered in Block 20, if different from Report)

18. SUPPLEMENTARY NOTES

19. KEY WORDS (Continue on reverse side if necessary and identify by block number)

Collision Decomposition of the negative ion of Uranium Hexafluoride

20. ABSTRACT (Continue on reverse side if necessary and identify by block number)

Absolute total cross sections for the collisional decomposition of the negative ion of uranium hexafluoride into its three lowest asymptotic channels in collisions with the rare gases were measured for collision energies ranging from below thresholds for decomposition up to a laboratory collision energy of 500eV. The experimental results were found to be consistent with the predictions of a two-step collision model where the unimolecular decomposition of the excited molecular negative ions is described with a statistical theory.

DD FORM 1473

UNCLASSIFIED

B. Research Objectives

Our contract entitled "A Study of the Collisional Dynamics for Collisions of UF_6^- with Atoms and Molecules" was in the area of experimental atomic and molecular physics. The central objectives of this research were

1) to obtain accurate information about how the UF_6^- ion decomposes when it undergoes collisions with vaious atoms and molecules;

2) to attempt to explain these results quantitatively, utilizing one of a number of current theories about the unimolecular dissociation of highly excited molecules;

3) to investigate how the decomposition processes depend upon the internal energy stored in the UF_6^- ion; and finally,

4) to develop and test a surface ionization source capable of producing intense beams of UF_6^-.

C. Status of the Research

The scientific approach employed in the experimental portion of this research is to produce a negative ion beam of UF_6^- at known energies and allow it to collide with a particular gas at low pressure. The various charged fragments produced by collisional decomposition are then identified by conventional means. By simply measuring the intensities for each fragment ion, the probability (i.e., the cross section) of producing a given fragment in a single collision can be obtained directly from such experiments.

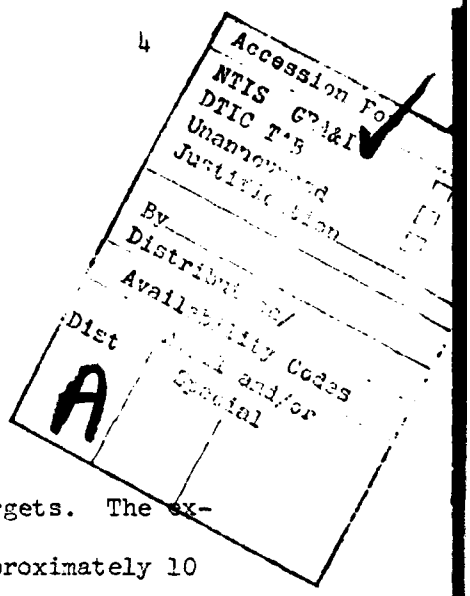

The cross sections for the decomposition channels:

$$UF_6^- + X \rightarrow UF_5 + F^- + X$$
$$\rightarrow UF_5^- + F + X$$
$$\rightarrow UF_6 + e + X$$

have now been measured with the inert gases, N_2 and SF_6 as targets. The experiments cover the laboratory collision energy range from approximately 10 to 500 electron volts.

These experiments show that the cross sections for the production of fast neutral UF_5 molecules become quite large at high energies for all targets studied. Therefore, these results indicate that it may be feasible to use such stripping or decomposition collisions for the generation of fairly concentrated neutral beams of fast-heavy molecules.

In addition to the completed experiments, considerable progress was made on a statistical theory which shows promise of being able to describe (or predict) quantitatively these complicated collision-induced decomposition processes.

The experimental results, along with detailed discussions of these measurements and calculations can be found in the attached draft manuscript. For those not wishing to consult the manuscript, a brief summary of the progress made during the contract period follows.

The research conducted during the past year led to some surprising results which we consider both important accomplishments and significant achievements.

Clearly when a complicated molecular ion such as UF_6^- collides with an atom or molecule at collision energies in excess of a few tens of electron

volts, many ways of dissociating or breaking up the molecular ion become energetically possible.

Based upon what is currently known (both experimentally and theoretically) about the quantum states of UF_6^-, the decomposition channel having the lowest binding energy (thought to be 4.3 ± .5 electron volts) is

$$UF_6^- \rightarrow UF_5^- + F.$$

we have measured the thresholds for this channel using different targets and found them to be in the neighborhood of 2 electron volts. The question arises as to why these thresholds are so low. There are several possible explanations; but at the moment, there is insufficient experimental information to clarify the situation. The UF_6^- ions were produced on a hot (1250K) surface; and if it is assumed that the desorbed UF_6^- is in thermodynamic equilibrium with the hot surface, one expects the UF_6^- to possess approximately 1.5 electron volts of internal energy. This means that an extra 1.2 electron volts is still needed to explain the observed threshold of 2 electron volts. Another possibility is that collisions between the UF_6^- ions and the parent gas UF_6 (as the UF_6^- is extracted from the ion source) lead to additional internal excitation of the UF_6^-. Alternately, the UF_6^- may not be produced in thermodynamic equilibrium with the hot surface.

Independent of what final explanation is correct, these threshold measurements are of considerable interest since they contain information about the internal energy distributions of the molecular ion in the primary beam.

One other result from this past years' efforts should be noted: the progress made in developing a statistical model to explain the experimental observations mentioned above. An example of some experimental results

showing the ratio of the probability (i.e., branching ratios) that UF_6^- breaks up into UF_5^- + F, to that for UF_6^- going to UF_5 + F^- is shown in the top figure on page seven. Results are shown for several different targets and indicate that this branching ratio is indepenedent of the target species but dependent upon the collision energy. The lower figure is a calculation of this branching ratio, based upon a particular statistical model which is discussed in the attached draft manuscript. The important thing to notice is that this ratio depends upon the relative collision energy (the experiment) and the internal energy of the UF_6^- just prior to decomposing (theory) in a remarkably similar manner. Moreover, the quantitative agreement between the two is very satisfying. All that remains is to understand the relationship between the abcissae of the two figures. We consider the progress reported here to be a major accomplishment in understanding the collisional decomposition of such complicated molecular systems.

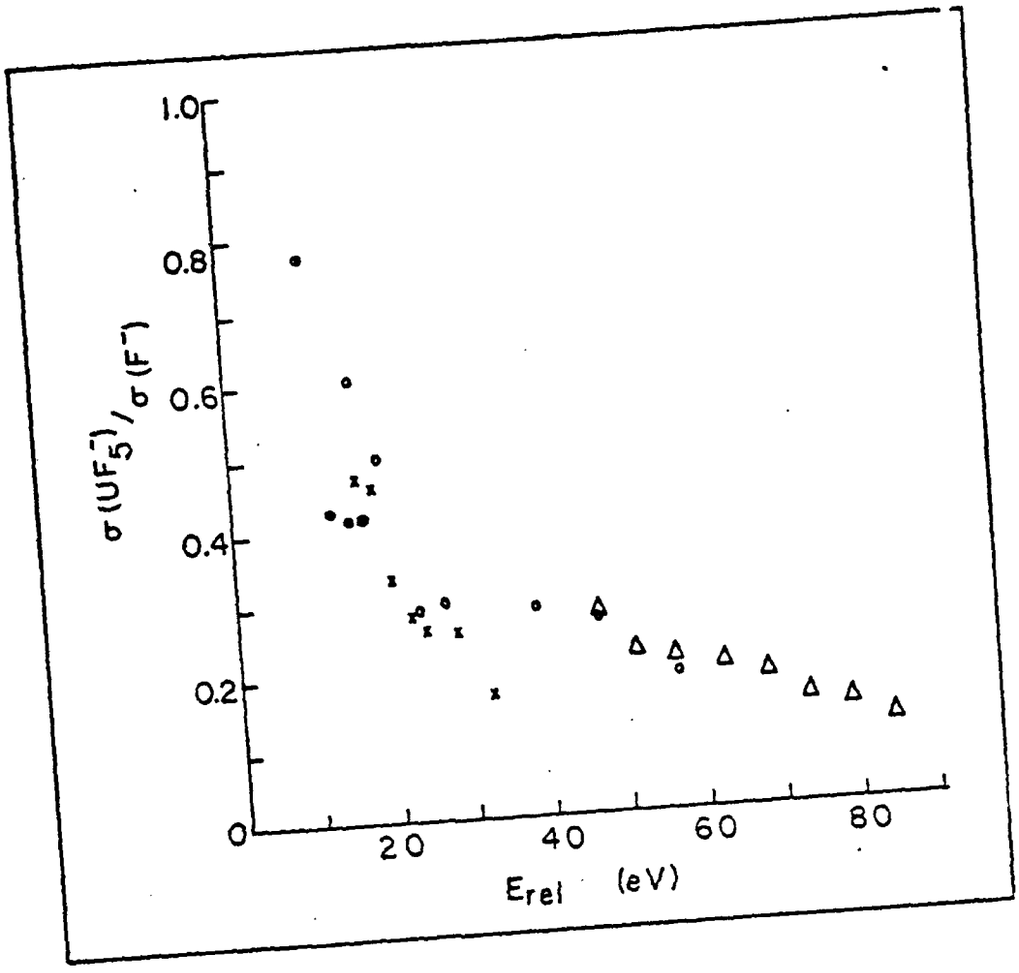

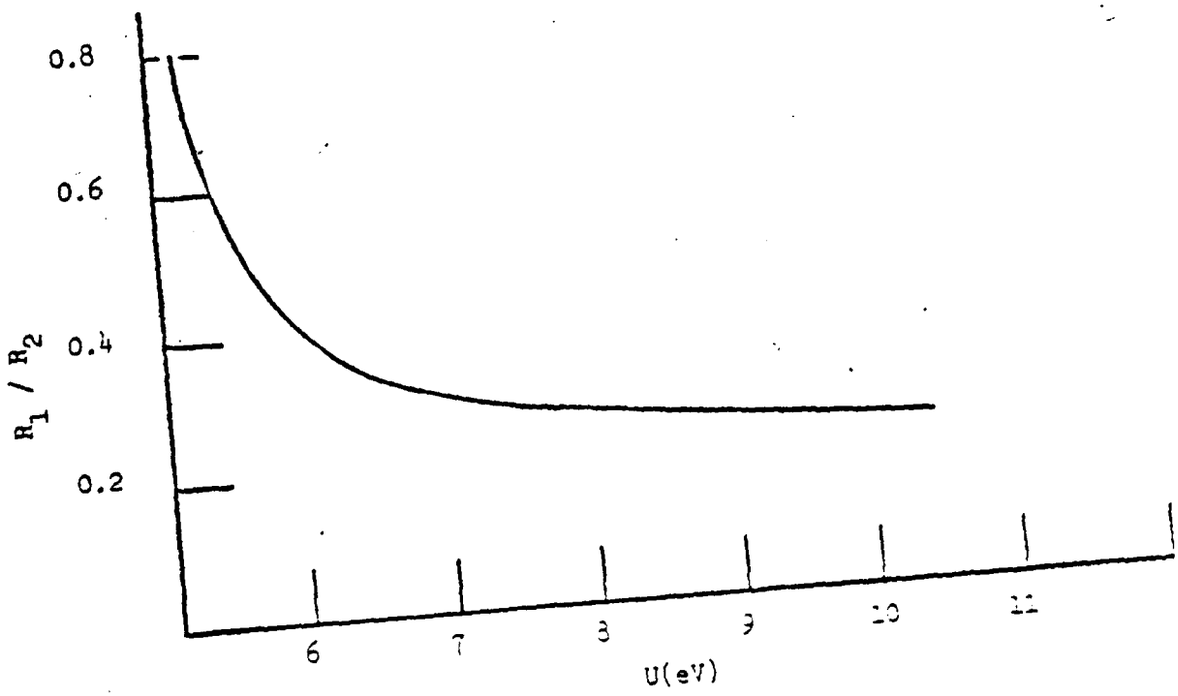

Branching ratio for E_{rot} = 1?? U.

D. Personnel Associated with Research Effort

The following personnel have been associated with the research effort at William and Mary:

S. E. Haywood	12 woman - months
L. D. Doverspike	2.5 man-months
R. L. Champion	2.5 man-months
E. Herbst	2 man-months

The first three persons were supported by the contract whereas E. Herbst contributed to the project but was not supported by the contract.

E. Appendix

The draft manuscript which follows will be submitted to the Journal of Chemical Physics. The manuscript contains the details of the work performed during the contract period.

DRAFT

COLLISION DECOMPOSITION OF UF_6^-

S. E. Haywood, E. Herbst, L. D. Doverspike and R. L. Champion

Department of Physics

College of William and Mary

Williamsburg, Virginia 23188

and

B. K. Annis and S. Datz

Chemistry Division

Oak Ridge National Laboratory

Oak Ridge, Tennessee 37830

ABSTRACT

Absolute cross sections for the collisional decomposition of UF_6^- into its three lowest asymptotic channels in collisions with the rare gases have been measured for collision energies ranging from below the threshold for decomposition up to a laboratory collision energy of 500 eV. The product velocity spectra have also been measured for one of the decomposition channels at the highest collision energy. The experimental results are found to be consistent with the predictions of a two-step collision model where the unimolecular decomposition of excited UF_6^- ions is described in a statistical framework.

I. INTRODUCTION

Because of interests ranging from the separation of uranium isotopes to the production of electronless plasmas uranium hexafluoride, UF_6, has been studied extensively both experimentally and theoretically.[1-12]. There is now substantial evidence from surface ionization[1], ion cyclotron resonance[2] and ion-neutral beam experiments[3-6] to establish that uranium hexafluoride has a large electron affinity. The studies to date are consistent with a lower limit of $\simeq$ 5eV for the electron affinity of UF_6. It is likely that molecules with such large electron affinities possess a number of electronically excited bound states of the molecular negative ion. Recent calculations suggest the existence of such excited states for UF_6^- which lie within 3 eV of the $^2A_{2u}$ ground state.[9-11]

Experiments[12] involving the collisional excitation of UF_6^- by rare gas and hexafluoride targets show that substantial amounts of excitation energy can reside in the negative ion, although the experiments do not reveal how this energy is distributed among the electronic, vibrational and rotational degrees of freedom of UF_6^-.

Very little information is available on how UF_6^- decomposes in collisions with gaseous targets. Clearly when a complicated molecular ion such as UF_6^- collides with an atom or molecule at collision energies in excess of a few tens of electron volts, many ways of breaking up UF_6^- become energetically possible. Fig. 1 contains an energy level diagram of some of the lowest lying decomposition channels.

The purpose of this paper is to report on recent measurements[13] of the absolute total cross sections for the decomposition channels

$$UF_6^- + X \rightarrow \begin{cases} UF_6 + e^- + X & (a) \\ UF_5 + F^- + X & (b) \\ UF_5^- + F + X & (c) \end{cases} \qquad (1)$$

where X is Ne, Ar, Kr, and Xe. The collision energies range from below the threshold for each channel (except c) up to 500eV laboratory energy: the thresholds for channels 1(a) and 1(b) have been determined. The experiments are carried out in an ion-beam, gas target apparatus. In addition, time-of-flight velocity spectra for channel 1(b), taken at the upper end of the energy range for UF_6^- and the rare gas targets at various scattering angles are also presented. The experimental observations are analyzed in terms of a two-step statistical model which employs the basic formulation of Klotz.[14]

In Section II a discussion of the experimental procedures is presented. Section III contains the experimental results and finally the model used in the analysis of the data is presented and applied to the experimental results in Section IV.

II. EXPERIMENTAL METHODS

The experiments were performed using two different types of apparatus. One, in which total cross section measurements were made, is located at the College of William and Mary and the other, in which the velocity spectra of the reaction products wereobtained, is a time-of-flight apparatus located at Oak Ridge National Laboratory. One aspect of these experiments which is common to both apparatuses is the UF_6^- ion source. Consequently, we will first discuss the characteristics of this ion source and follow with a brief description of the separate apparatuses.

A. Ion Source

The design of the UF_6^- source is based upon recent experiments of Dittner and Datz[1] in which they observed that UF_6 desorbed from a hot filament as a negative ion with a conversion factor (i.e., the ratio of the negative ion flux desorbing from the filament to the neutral flux which is incident upon the filament) which approached unity. Moreover, this conversion factor was observed to remain near unity over a wide temperature range, $500K \lesssim T \lesssim 2000$ K. This phenomenon is reasonable because the electron affinity of UF_6 (about 5.1eV) is greater than the work function of the filament material. Thus, "surface attachment" for UF_6 molecules is an exoergic process. One further and crucial constraint is necessary, however, in order to achieve the unit conversion efficiency just mentioned: the surface of the

filament must be such that the UF_6 molecules are not lost due to competing processes which may occur on the surface such as $UF_6 \rightarrow UF_5 + F$, etc. A suitable "inert" surface was effected by using a platinum filament in a background gas of C_2H_2 (acetylene). The surface is presumably carbon-like.

The ion sources employed in the present experiments used a platinum filament at a temperature of about 1230K (as determined by an optical pyrometer) and a roughly equal mixture of C_2H_2 and UF_6 in the source chamber. Negative ion beams produced with this arrangement are both stable and intense. The total pressure within the ion source was not measured directly but is estimated to be in the neighborhood of about 10 microns. This estimate is based upon pressure measurements of the gas inlet tube on the upstream side of the actual source chamber. Due to the relatively high pressure within the source, some of the extracted UF_6^- ions may undergo inelastic collisions with the source gas before they reach the region of high vacuum (10^{-6} torr) which is external to the ion source. The possible manifestations of such "collisional pumping" will be discussed after the experimental results are presented.

B. Total cross section apparatus

The apparatus used to measure the various absolute total cross sections for reactions (1) is only slightly modified from the one used in previous negative ion studies and is discussed in detail in reference 15.

After the negative ion beam is extracted from the surface attachment ion source described above, it is accelerated and passes through a

filter and is subsequently focused into the collision chamber which contains the target gas; a schematic diagram of this chamber is given in Fig. 2. By varying electrostatic and magnetic fields within this collision chamber, it is possible to separate and measure the absolute total cross section for the three distinct reaction channels which are given in Eq. (1).

The collisional detachment (a) is measured by applying an axial (i.e., along the beam axis) magnetic field of several gauss along with a small electrostatic field between grids I and II (see Fig. 2) to serve as an electron trap: all detached electrons must eventually be collected by the element A. The heavy F^- ions from reaction (b) will not be affected by the axial magnetic field and some of those ions also arrive at element A. In order to separate the electron current from the F^- current, the magnetic field is rotated 90°: this will not affect the trajectories of the heavy negatively charged paricles but will prevent any electrons from reaching element A. Thus, the total electron current and hence the total detachment cross section can be ascertained. The initial UF_6^- beam current, the scattering path length and the number density of scattering centers are known and the cross section is unambiguously determined with an uncertainty estimated to be no more than 10%.

In order to discuss the measurement for channels (b) and (c), it is useful to assume that the dynamics of the collision-induced-dissociation (CID) channels (reactions (b) and (c) above) can be qualitatively described by a two step process:

$$\begin{aligned} UF_6^- + X &\rightarrow (UF_6^-)^* + X \\ &\quad\;\; \vdash\!\!\rightarrow UF_5 + F^- \\ &\quad\;\; \vdash\!\!\rightarrow UF_5^- + F, \end{aligned} \qquad (2)$$

where the asterisk implies that $(UF_6^-)^*$ has been collisionally excited and contains sufficient internal energy so that the dissociation is energetically possible. The products of CID then have roughly the same velocity in the laboratory reference frame but quite different kinetic energies. It is this latter feature which allows one to separate channels (b) and (c).[16] For example, if the laboratory energy of the projectile UF_6^- is E_1(eV), then the laboratory K.E. for F^- resulting from CID will be about $E_1/17$. Consequently, if the voltage on grid II (see Fig. 2) is, say $E_1/8$ (volts) then all of the F^- which is due to CID will be reflected by that electric field and collected on elements A and B. The result of a "retardation analysis" is shown in Fig. 3(a). The observation of a plateau region clearly indicates that the reflection of the F^- ions is complete. Thus the CID cross section for (b) may be determined. The cross section for (c) may also be measured in a similar fashion by varying the retardation voltage and observing the current which is transmitted through the retarding grids and collected on element C.

It is clear that the measurements can not unambiguously identify and separate the various heavy (charged) reaction products. Moreover, the simple two-step model which is used to discuss the kinematics of CID is probably overly simplistic. Nevertheless, any plausible modification of this model would not result in any substantial alteration in the kinematics of CID. Based upon the assumption that (b) and (c) are the sole products of CID, then the measurements for (b) and (c) should be accurate to within 10% and 30%, respectively. The larger error for (c) is due to the fact that the larger retarding voltages which are necessary to separate (c) from elastic scattering (or the primary ion beam) cause a substantial defocussing of

the ion beam which in turn makes the identification of "breaks" in the retardation analysis difficult to measure. Such a retardation is seen in Fig. 3(b).

The laboratory energy of the primary ion beam is determined by a retardation analysis similar to that shown in Fig. 3(b), but with no target gas in the chamber. The scattering chamber is housed in a differentially pumped section which is well isolated from the ion source region. This arrangement minimizes UF_6 intrusion into the collision chamber and no appreciable error due to contact potentials should be present. The laboratory energy should be accurate to within 0.25eV which translates into a very small error in the relative collision energy for the reactants studied.

C. Time of Flight Apparatus

(ORNL)

III. RESULTS

A. Electron Detachment Cross Sections

The absolute electron detachment cross sections for collisions of UF_6^- with the rare gases Ne, Ar, Kr, and Xe have been measured from threshold to a laboratory energy of 500 eV and the results are presented in Fig. 4. All the cross sections have the same general shape; each shows a threshold in the vicinity of 5eV (their threshold behavior will be discussed in detail later) then rise to a local maximum at a relative collisional energy around 15eV. Above 15eV the cross sections decrease, and each (except for Ne) possesses a local minimum near 30eV. Afterwards they increase monotonically with increasing collision energy. The low energy maximum in the cross section becomes more pronounced as the target mass increases, being almost indiscernable in the case of Ne.

This particular structure in the detachment cross section near threshold which is essentially independent of the target species is not understood at present. It should be noted that the detachment cross sections are remarkably small even at relative energies of 100eV.

B. Dissociation Channels

Absolute cross sections for the dissociation channels 1(b) and 1(c) were determined for the rare gas targets and same range of collision energy as for detachment. Cross sections for the production of F^-, $\sigma(F^-)$, are

presented in Fig. 5 while the ratio $\sigma(UF_5^-)/\sigma(F^-)$ rather than $\sigma(UF_5^-)$ is shown in Fig. 6. An interesting feature in Fig. 6, is that the ratio $\sigma(UF_5^-)/\sigma(F^-)$ is independent of the target and is an approximately universal function of the relative collision energy. Channel 1(b), although more endoergic than 1(c), is clearly the dominant process at elevated energies with 1(c) becoming relatively important only in the threshold region. The data in Fig. 5 show that $\sigma(F^-)$ rises rapidly from a threshold in the vicinity of 2.5eV then reaches a plateau for $E_{rel} \simeq$ 20-25eV. The cross sections also systematically increase with the mass of the target atom. From these results it is clear that electron detachment is a minor contributor to the collisional destruction of UF_6^- in the energy range investigated.

Threshold Measurements

The threshold region for reactions 1(b) was studied in detail for all the rare gas targets. Experimental limitations discussed earlier prevented similar measurements on channel 1(c), while the smallness of the detachment cross sections limited the accuracy of threshold studies for this channel.

An expanded view of the measurements in the threshold region for channels 1(a) and 1(b) is shown in Fig. 7. For both channels the square roots of the cross sections are plotted versus relative collision energy, and it is clear the plots are quite linear over the range of energies shown. A linear extrapolation of $\sqrt{\sigma(F^-)}$ to zero cross section indicates that the threshold for channel 1(b) is approximately 2eV for all targets while the

same procedure for the detachment channel 1(a) is consistent with a threshold in the vicinity of 4-5 eV.

The observed threshold for process 1(b) is considerably below the currently accepted value of 4.7eV shown in Fig. 1. There are several reasons for expecting the threshold determined in the present experiments to be lower. To begin with the UF_6^- is produced by desorbtion from a hot filament and therefore will possess a significant amount of internal energy if it is in thermal equilibrium with the filament before desorbtion. All the data shown in this paper were taken at a filament temperature of 1230K as determined by an optical pyrometer. Assuming the UF_6^- is in thermal equilibrium with the filament at temperature T, it then follows that the mean internal energy of the desorbed ions is

$$\bar{U} = 3/2 \cdot RT + \sum_{i=1}^{15} h\nu_i \Big/ \left(e^{h\nu_i/kT} - 1\right) \qquad (3)$$

where the first term is the rotational contribution and the second is the energy in vibration. Using the estimates of Compton[3] for the vibrational frequencies, ν_i, of UF_6^-, gives $\bar{U}$ = 1.5eV at a temperature of 1230 K. Assuming that UF_6^- contains this amount of internal excitation one still needs an additional 1.2eV in the form of internal excitation to explain the observed threshold for 1(b). The experimental data have been corrected for thermal[18] and apparatus broadening by employing a numerical deconvolution scheme used in the analysis of previous threshold measurements[19] of collisional detachment cross sections. The effect of removing the broadening from the

present data is quite small. The thresholds would be lowered by only about 0.1eV and, therefore can not account for the 1.2eV. The additional energy is most likely due to "collisional pumping" of the UF_6^- as it is extracted from the surface source. The extraction electrode extends approximately 2cm inside the source chamber and is normally maintained at +100 volts with respect to the filament and source chamber. With the present arrangement the source gas pressure is roughly the same throughout this region; the pressure although not measured directly in the source, is probably high enough to make collisions between the extracted UF_6^- and UF_6 likely in the extraction region. Recent studies by Annis and Stockdale[12] show that UF_6^- when scattered by various targets (including UF_6) possess internal energies of several eV, which is presumably in vibrational modes. As the vibrational relaxation is slow compared to the transit time in the present experiments ($\sim 10\,\mu$sec), these collisionally excited UF_6^- ions are in the ion beam and are probably responsible for the low threshold observed. As can be seen in Fig. 7, the threshold for detachment is found to be several eV higher than that for F^- produced via CID, although the asymptotic states for the two channels are separated by only 0.5eV. It will be shown later that this observation is compatible with the prediction of a statistical model that the lifetime for detachment of UF_6^{-*} is greater than the transit time within the collision chamber ($\sim 1\mu$sec) for low relative collision energies, in contrast to the prediction for CID.

C. Velocity Spectra

Velocity spectra of the energetic neutral products of collisional decomposition were measured at a laboratory energy of 500eV for laboratory scattering angles $\Theta \leq 3.5^{\circ}$. The particle detector in the time-of-flight apparatus would only detect UF_6 from 1(a) or UF_5 from 1(b): F from 1(c) would not be detected because of its low laboratory kinetic energy (approximately 30eV). Since the total cross section for detachment is only a few per cent of that for CID, the neutral TOF spectra essentially reflect the velocity spectra for channel 1(b). An example for the Ar target is shown in Fig. 8 for a laboratory scattering angle of 1.5°. The scale at the top of the graph gives the endothermicity, Q, calculated from the observed delay time for the UF_5 molecules and is based upon the assumption of the two-step model:

$$\begin{aligned} UF_6^- + Ar &\rightarrow UF_6^{-*} + Ar + Q \ , \\ UF_6^{-*} &\rightarrow UF_5 + F^- , \end{aligned} \qquad (4)$$

where in the second step the CID products separate from each other with zero relative velocity and have a negligible post-excitation interaction with the neutral target atom.

If the CID products separate with non-zero momenta in an isotropic manner, then the net effect will generally be to broaden the velocity spectrum rather than to shift its centroid an appreciable amount. Hence the centroid of the distribution in Fig. 8 which yields $\bar{Q} \simeq -5$eV should be the endothermicity of the first step of CID if the assumptions of the two-step model are

compatible with the reality of the collisional dynamics.

If $\bar{Q} \simeq$ -5eV, then the internal energy, $\bar{U}$, of UF_6^{-*} for those molecular ions which ultimately decompose to $UF_5 + F^-$ is the sum of the internal energy prior to the collision and the five eV transferred by the collision. If the original internal energy of the UF_6^- projectile is about 2 eV (as indicated by the threshold behavior of the total CID cross section) then it follows that $\bar{U} \simeq$ 7eV for reaction 1(b) to occur. This result is compatible with the internal energy necessary to produce the observed CID branching ratio as predicted by the statistical theory to be discussed later. The velocity spectra taken with other targets are essentially the same as that shown in Fig. 8. The observed $\bar{Q}$'s are also approximately independent of scattering angle and only a broadening of the velocity spectra is observed with increasing scattering angle.

IV. THEORETICAL TREATMENT

We shall again assume that the collision-induced dissociation of UF_6^- can be approximated as the two-step process

$$UF_6^- + X \rightarrow UF_6^{-*} + X$$

$$UF_6^{-*} \rightarrow \text{products}$$

where X is a rare gas target. The first step is a strongly inelastic collision in which sufficient energy is transferred from the relative collision energy E_{rel} into internal energy of UF_6^- so that the molecule is excited into its quasi-bound ro-vibrational levels above at least the first dissociation limit. The second step is the subsequent dissociation of the UF_6^{-*} "complex". This description has meaning if the "complex" lifetime is greater than the collision time. The treatment here is concerned solely with the spontaneous decomposition of UF_6^{-*} molecules with known internal energy U and angular momentum quantum number J_o. We are able to calculate the UF_6^{-*} decomposition frequencies and relative strengths for the products channels, or branching ratios, as functions of U and J_o. We have not attempted to calculate the U and J_o distributions of UF_6^{-*} species to be expected from UF_6^- - X collisions at known values of E_{rel} involving UF_6^- molecules of initial U, J_o distributions.

Excited UF_6^- molecules can dissociate into three low-lying product channels as illustrated in Fig. 1:

$$i = 1 : UF_6^{-*} \rightarrow UF_5^- + F \quad ---- \quad U_{0,1} = 4.3 \pm 0.5 \text{ eV}$$

$$i = 2 : UF_6^{-*} \rightarrow UF_5 + F^- \quad ---- \quad U_{0,2} = 4.7 \pm 0.3 \text{ eV}$$

$$i = 3 : UF_6^{-*} \rightarrow UF_6 + e \quad ---- \quad U_{0,3} = 5.2 \pm 0.5 \text{ eV}$$

where the $U_{0,i}$ represent threshold internal energies and are taken from experimental sources.[2,3] The experimental uncertainties in the $U_{0,i}$, though large, are not all independent. The decomposition frequencies $k_i(U,J_o)$ of UF_6^{-*} molecules into product channels, i, can be obtained conveniently from the statistical ("quasiequilibrium") theory of Klotz[14]. For the case in which a molecular spherical (or near spherical) top dissociates into a molecular spherical (or near spherical) top and an atom (or electron), Klotz's expression for the decomposition frequency is

$$k_i(U,J_o) = \frac{\alpha_i}{h(2J_o+1)\,\rho_{vib}^{UF_6^{-*}}(E_{vib})} \int_{\chi=0}^{U_i = U-U_{o,i}} \rho_{vib}^{Prod}(\chi) \sum_J \sum_L (2J+1)\, d\chi \qquad (5)$$

where h is Planck's constant; $\rho_{vib}^{UF_6^{-*}}$ is the vibrational density of states of UF_6^{-*} at vibrational energy E_{vib}; χ, $\rho_{vib}^{Prod}(\chi)$, and J are the vibrational energy, vibrational density of states and rotational angular momentum quantum number of the product spherical top molecule; L is the orbital angular momentum quantum number of the products; and α_i is the ratio of the symmetry numbers of UF_6^- and the product spherical top. The density of vibrational states of a polyatomic molecule can be approximated accurately by the analytic formula of Whitten and Rabinowitch[19]. Because ρ_{vib} is such a strong function of energy, excited electronic states of UF_6^- and products need not be considered in our analysis because their vibrational densities of states at any given total energy are smaller than those of the respective electronic ground states. This simplification is central to the analysis since the species involved have many low-lying excited electronic states.

The restrictions on the angular momentum quantum numbers J and L in Eq (5) are determined as follows. For the spherical top-atom channels (i = 1,2), once a value of χ is chosen, the rotational energy E_{rot} of the product spherical top can range from 0 to $U - U_{o,i} - \chi$. Since

$$E_{rot} = B \cdot J(J+1) \tag{6}$$

for a spherical top where B is the rotational constant, the range of J is thereby defined. The range of L (if any) is defined by the triangle rule $|J-J_o| \leq L \leq J+J_o$ and the Langevin (polarizability) restriction on L_{max}[14]. For the detachment channel, only s-and p- electrons contribute appreciably so that L = 0,1 and $J = J_o \pm 1$, where J_o is the UF_6^{-*} angular momentum quantum number.

Necessary inputs for the calculations of k_i are the threshold energies $U_{o,i}$[2,3]; the harmonic oscillator frequencies,[3,20] rotational constants[3] and symmetry numbers[3,20] of UF_6^-, UF_5^- and UF_5, and the dipole polarizations of UF_5 and F.[21] The uncertainties in these parameters are often severe. For example, some of the UF_6^- harmonic oscillator frequencies are obtained by assuming them to equal those of the isoelectronic species NpF_6 whereas the UF_5^- frequencies are assumed to equal those of UF_5. Thus even if Eq (5) were exactly correct, the various calculated values of k_i would be highly uncertain. Once the $k_i(U,J_o)$ have been determined, the branching ratios R_i can be obtained from the formula

$$R_i = k_i / \sum_j k_j \tag{7}$$

assuming the k_i to be sufficiently large that decomposition can be detected.

We have computed $k_i(U,J_0)$, i = 1,2,3 numerically for internal UF_6^{-*} energies under 15 eV and a variety of angular momenta. Fig. 9(a) depicts the $k_i(U,J_0=0)$. The dissociation frequencies shown are strongly dependent on internal energy, ranging from less than 10^5 sec^{-1} near threshold to 10^{14} sec^{-1} at 15 eV. Note that the detachment channel is correctly predicted to be a minor one. The computed values of $k_i(U,J_0)$ are also dependent on J_0. Increasing J_0 tends to decrease the dissociation frequencies, especially near threshold.

To compare our theoretical and experimental results, we have calculated the branching ratios R_i. For all values of angular momentum considered, R_3 (the detachment channel branching ratio) is $\lesssim 0.01$ and increases with increasing energy. This is in qualitative agreement with experiment. However, the actual numerical values appear to be lower than experimental values for any reasonable assumed internal energy distributions of UF_6^{-*}. The ratio of channel 1 (UF_5^-) to channel 2 (F^-) products as a function of E_{rel} is a salient feature of our experimental results. The theory can "reproduce" this feature if it is reasonably assumed that the UF_6^{-*} rotational energy is a fixed percentage of total internal energy. In Fig. 10(a), we have plotted calculated values of $k_i(U,J_o)$ assuming E_{rot} to be held fixed at 17% of the internal energy U. In Fig. 10(b) the ratio R_1/R_2 is then plotted against UF_6^{-*} internal energy with rotational energy $E_{rot}=0.17U$. Note that the ratio decreases strongly at energies close to threshold ($\simeq$ 6eV) and then levels off. The analogous experimental plot shows a similar dependence of $\sigma(UF_5^-)/\sigma(F^-)$ on collision energy E_{rel}. In this plot (Fig. 6) the leveling off occurs at $E_{rel} \simeq$ 15-20eV. One would expect the plot of the above ratio vs. internal energy of UF_6^{-*} to be sharper than Fig. 6 because the range of UF_6^{-*} internal energies for any collision energy will certainly lie below E_{rel}. The exact shape of the theoretical curve is a function of

the percentage of total internal energy of UF_6^{-*} assumed to be rotational energy. Still, for E_{rot} equal to a variety of fixed percentages of U, the qualitative feature remains - the ratio of UF_5^- to F^- products decreases with increasing U at first sharply and then more slowly (until $U \simeq 9$eV at which secondary decomposition of UF_5^- occurs). Despite the wide uncertainties in the parameters used in the calculations, this reproduction of the experimental feature must be regarded as a success of the theory. It stems from two facets of the calculation - at lower energies the lower threshold energy of $UF_5^- + F$ production dominates whereas at higher energies the higher polarizability of UF_5 (compared with F) results in more $UF_5 + F^-$ states being "counted" in Eq. (5). The absolute R_1/R_2 predictions, though tantalizingly close to the experimental branching ratios, for $E_{rot} = 0.17U$ and any reasonable U-distribution, should not be taken as seriously.

Finally, the theoretical results show that the threshold for detachment is larger by several eV than the threshold for CID. The transit time in the collision chamber of the total cross section apparatus is $\sim$1μsec. Consequently, the value of k_i for any channel must reach $\sim 10^6 sec^{-1}$ before products can be detected. Depending on the amount of angular momentum possessed by UF_6^{-*}, the decomposition frequency for detachment reaches this value at internal energies U of 1.5-3.0eV in excess of the CID channels. If E_{rot} is once again held fixed at 17% of U, the figure is $\sim$ 2.75eV. This is in good agreement with the threshold experimental results depicted in Fig. 7 where CID onsets at a collision energy of 2-3eV below detachment.

V. SUMMARY

Measurements of the absolute total cross sections for collisional decomposition of UF_6^- into its three lowest-lying asymptotic channels have been made for collision energies ranging from below threshold up to 500 eV laboratory energy. The targets used in the experimental studies were the rare gases Ne, Ar, Kr, and Xe. In addition the product velocity spectra for one of the decomposition channels have been determined for the highest collision energies.

The salient features of the experimental findings are: (i) the cross sections for the collisional electron detachment of UF_6^- are quite small and are no more than a few percent of the total decomposition cross sections over the range of energies investigated; (ii) the cross sections for the less endoergic dissociation channel (UF_5^- + F) are smaller than those for the channel (UF_5 + F^-) for relative collision energies above about 10 eV; (iii) the general features of all the cross sections - when plotted as a function of the relative collision energy - are independent of which rare gas target is involved; (iv) the threshold energy for electron detachment is about 2-3eV greater than that for the dissociation channel (UF_5 + F^-); (v) the velocity spectra indicate that the collision which leads to the principal decomposition channel (UF_5 + F^-) is most probably several eV more endoergic than the minimum endoergicity required for the dissociation to occur.

These results have been analyzed with a two-step collision model where collisional excitation of UF_6^- is followed by unimolecular decomposition which is target independent. The branching ratios for the unimolecular decomposition have been calculated by using a statistical formulation which has been discussed previously by Klotz[14]. Although the details of the original collisional excitation of UF_6^- are not incorporated in the model, the statistical predictions for unimolecular decomposition are in surprisingly by good agreement with the experimental observations.

REFERENCES

1. P. F. Dittner and S. Datz, J. Chem. Phys. 68, 2451 (1978)
2. J. L. Beauchamp, J. Chem. Phys. 64, 939 (1976)
3. R. N. Compton, J. Chem. Phys. 66, 4478 (1977)
4. B. P. Mathur, E. W. Rothe and G. P. Reck, J. Chem. Phys. 67, 777 (1977)
5. B. K. Annis and S. Datz, J. Chem. Phys. 69, 2553 (1978)
6. J. A. D. Stockdale, R. J. Womack and R. N. Compton, Chem. Phys. Lett. 63, 621 (1979)
7. M. Boring, J. H. Wood and J. W. Moskowitz, J. Chem. Phys. 61, 3800 (1974)
8. M. Boring, Chem. Phys. Lett. 46, 242 (1977)
9. P. J. Hay, W. R. Wadt, L. R. Kahn, R. C. Raffenetti, and D. H. Phillips, J. Chem. Phys. 71, 1767 (1979)
10. D. D. Koelling, D. E. Ellis, and R. J. Bartlett, J. Chem. Phys. 65, 331 (1976)
11. M. Boring and J. H. Wood, J. Chem Phys. (to be published)
12. B. K. Annis and J. A. D. Stockdale, (submitted to J. Chem. Phys.)
13. A portion of the present work was reported on previously: R. L. Champion, L. D. Doverspike, E. Herbst, S. Haywood, B. K. Annis and S. Datz, XI th ICPEAC, Kyoto, 1979; p. 618 of Abstracts of Contributed Papers.
14. C. E. Klotz, J. Phys. Chem. 75, 1526 (1971); A. Naturforch. 27A, 553 (1972); J. Chem. Phys. 64, 4269 (1976); Chem. Phys. Lett. 38, 61 (1976)
15. B. T. Smith, W. R. Edwards, L. D. Doverspike and R. L. Champion, Phys. Rev. A18, 945 (1978)
16. The assumptions associated with this rather simple model have been discussed previously. See, e.g., E. Herbst, K. A. Mulholland, R. L. Champion and L. D. Doverspik J. Chem. Phys. 67, 5074 (1977)
17. [illegible]

18. P. J. Chantry, J. Chem. Phys. 55, 2746 (1971)

19. G. Z. Whitten and B. S. Rabinowitch, J. Chem. Phys. 41, 1883 (1964)

20. B. J. Krohn, W. B. Person and J. Overand, J. Chen. Phys. 65, 969 (1976)

21. R. R. Teachout, R. T. Pack, At. Data 3, 195 (1971); National Bureau of Standards Circular 537 (1953). The polarizibility of UF_5 is approximated to be equal to that of UF_6.

Figure Captions

Figure 1 Energy level diagram for the lowest decomposition channels of UF_6^-. The values are in electron-volts and were obtained from references 2 and 3.

Figure 2 Schematic diagram of the collision chamber region. Grids labeled I, II, III are 95% transparent. By using grids II and III to provide retarding electrostatic fields and by applying either an axial ($B_{//}$) or transverse ($B_{\perp}$) magnetic field, the three decomposition channels in Eq (1) can be identified.

Figure 3 (a) Retardation analysis for F^-; The ordinate gives the current to elements A and B as a function of a retarding voltage applied to grids II and III for the Xe target and a laboratory energy, E_1, of 40eV. The arrow at $V \simeq E_1/17$ is the mean energy (in eV) for F^- expected from simple CID considerations.

(b) Retardation analysis for UF_5^-. The ordinate gives the current to element C as a function of the retarding voltage for the Ar target with E_1 = 278eV. The arrow at $V \simeq 16(E_1-5)/17$ is the mean energy (in eV) for UF_5^- expected from simple CID considerations and an endothermicity of 5 eV in the original excitation process. The uppermost curve is a retardation plot for UF_6^- with no target gas in collision chamber.

Figure 4 Absolute total detachment cross section for UF_6^- + rare gases as a function of the relative collision energy: Δ- Xe; 0 - Kr; X - Ar; ● -Ne.

Figure 5 Absolute total cross section for CID of UF_6^- by the rare gases as a function of the relative collision energy: Δ -Xe; 0-Kr; X - Ar; ● -Ne.

Figure 6 Branching ratio for the two CID channels, where R = $\sigma(UF_5^-)/\sigma(F^-)$, as a function of the relative collision energy: Δ -Xe; 0 - Kr; X - Ar; ● -Ne.

Figure 7 Threshold behavior of $\sigma(F^-)$ and the detachment cross section. The square root of the cross sections are plotted as a function of the relative collision energy. (F^-): Δ - Xe; 0 - Kr; X - Ar; ● - Ne. Detachment ▲ - Xe; □ - Kr; ⊗ - Ar. The square root of the detachment cross section has been multiplied by two for display purposes.

Figure 8 Time of flight spectrum of UF_5 produced by UF_6^- in Ar for a laboratory energy of 500eV and a laboratory scattering angle of 1.5°. Solid curve is UF_5 and the dashed curve is the primary beam, UF_6^-, profile. Also shown is the endothermicity, -Q, for this process, determined by assuming that the CID can be described by a two step model, See text for discussion of the two step model.

Figure 9 Calculated decomposition frequencies $k_i(U,J_o=0)$ are plotted as a function of the internal energy, U, for channels i = 1 (UF_5^- + F), i = 1' (UF_5^- + F, allowing for secondary decomposition of UF_5^-), i = 2 (UF_5 + F^-), and i = 3 (UF_6 + e).

Figure 10 (a) Calculated decomposition frequencies $k_i(U,J_o)$ for E_{rot} = 0.17U. See Fig. 9 for an explanation of the symbols. Note that for k $10^6 sec^{-1}$, the internal energy necessary for detachment is 2.7eV greater than that for CID.

(b) The branching ratio between channels 1 and 2 above as a function of internal energy for E_{rot} = 0.17 U.

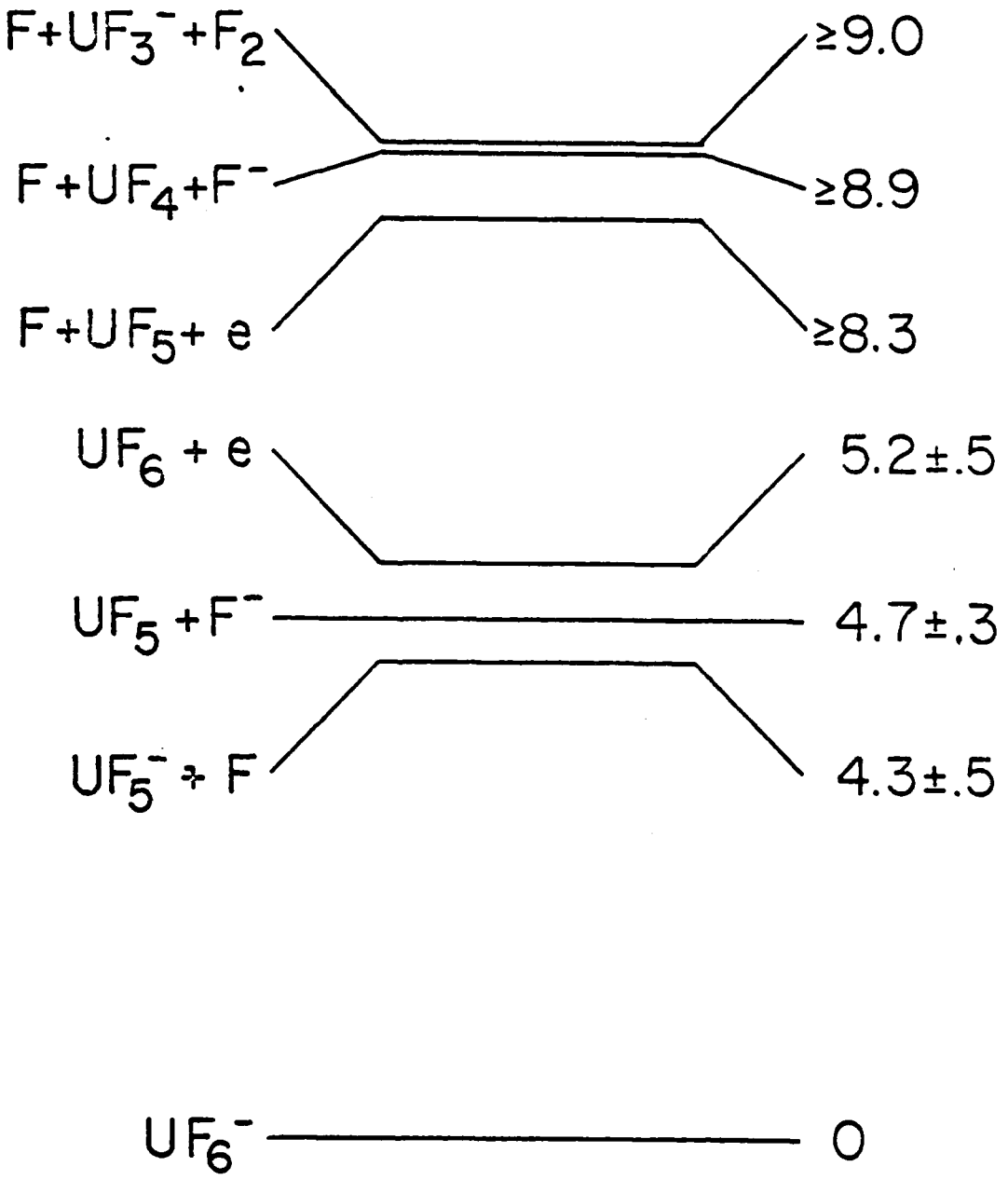

Fig. 1

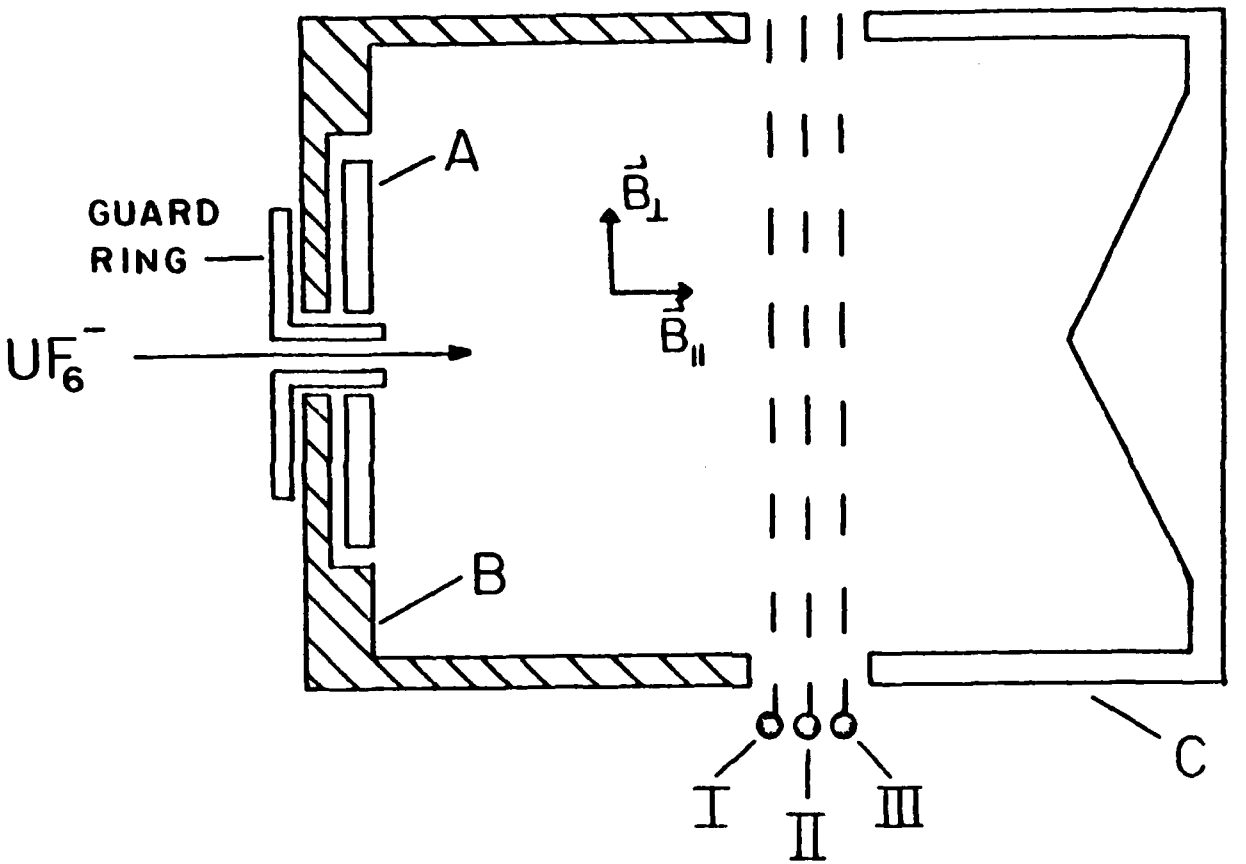
A
GUARD
RING
$\vec{B}_\perp$
$\vec{B}_\parallel$
UF_6^-
B
C
I
II
III

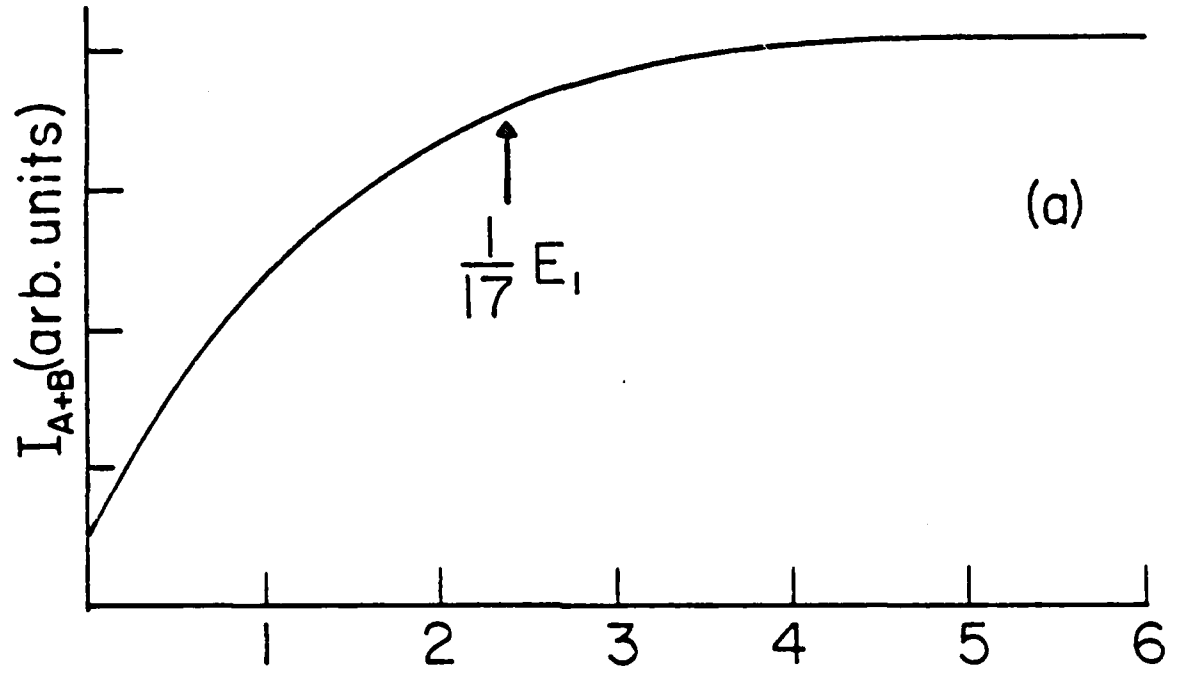
I_{A+B}(arb. units)
$\frac{1}{17}E_1$
(a)
1
2
3
4
5
6

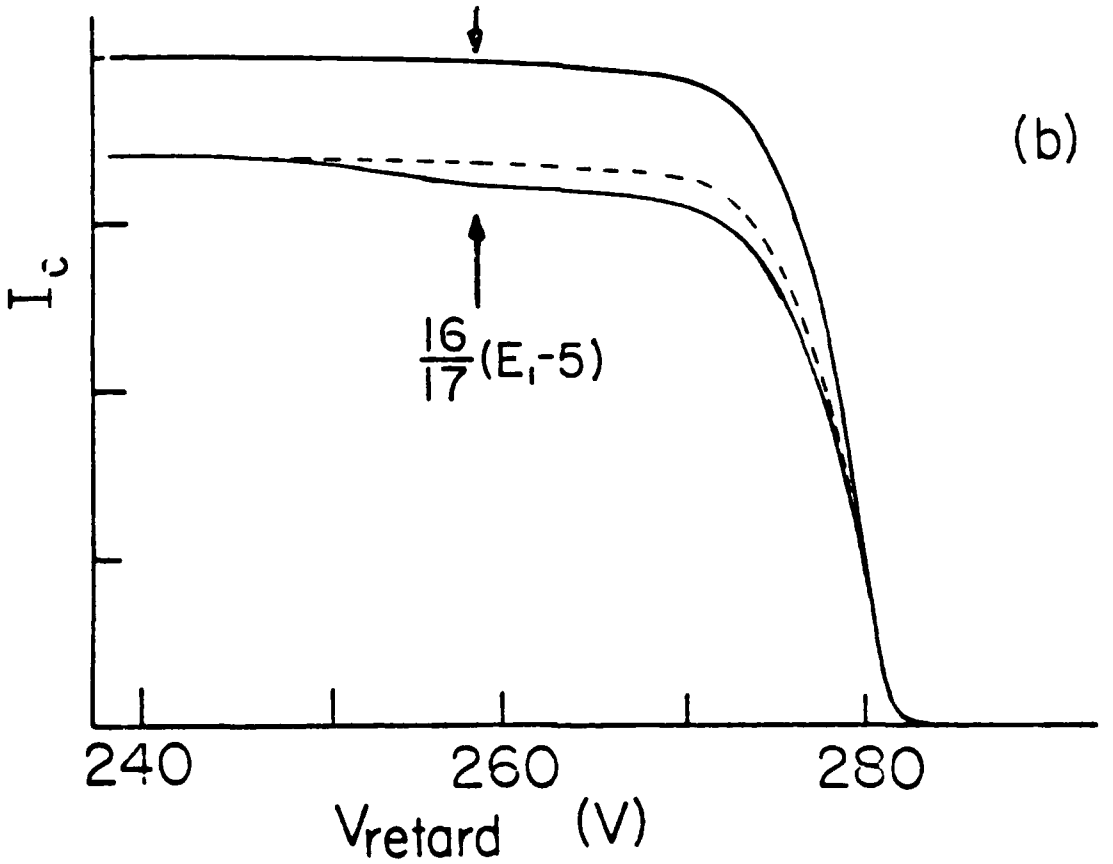
I_c
$\frac{16}{17}(E_1-5)$
(b)
240
260
280
Vretard (V)

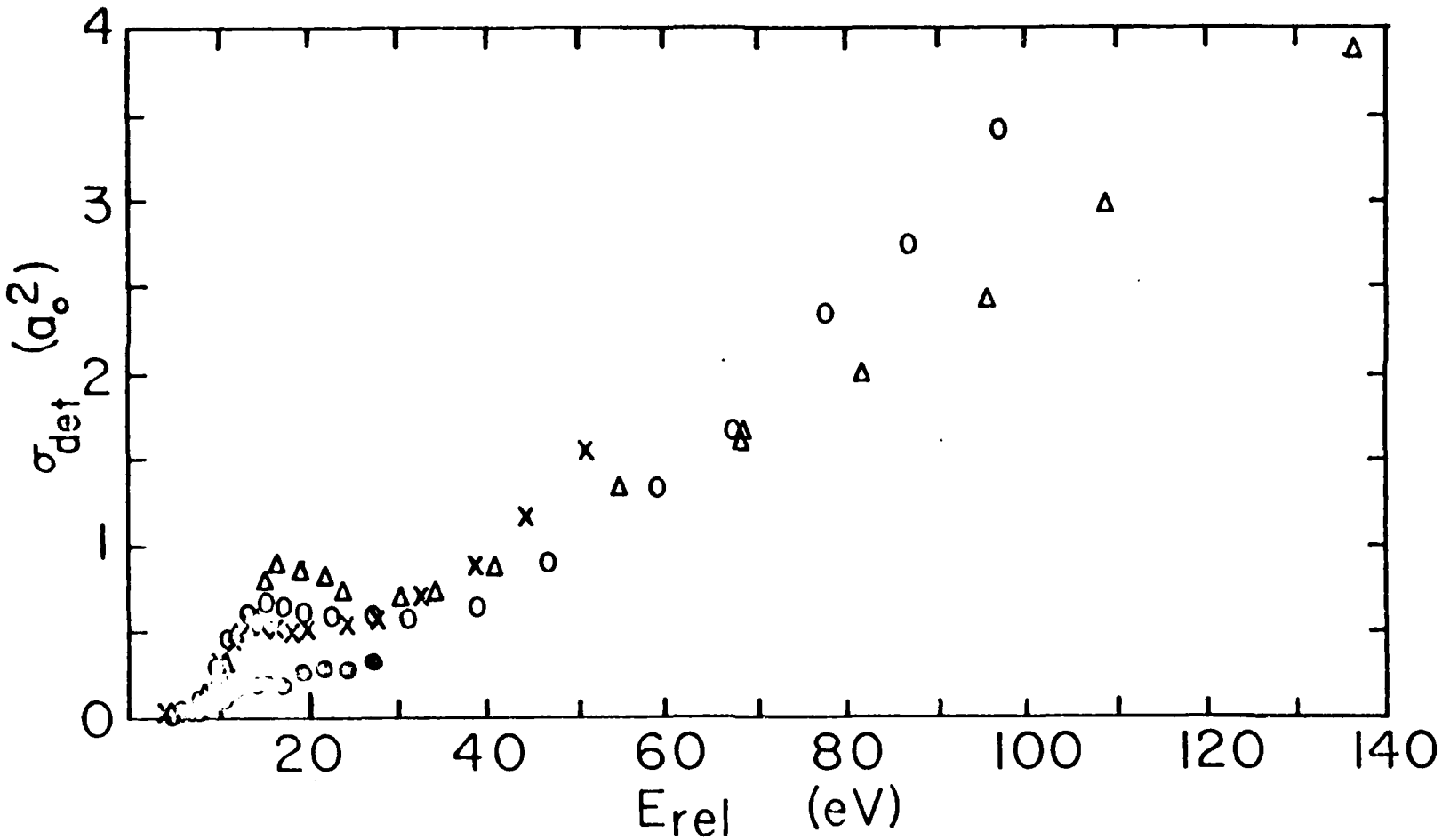
4
3
2
1
0
σ_{det} (a_o^2)
20
40
60
80
100
120
140
E_{rel} (eV)

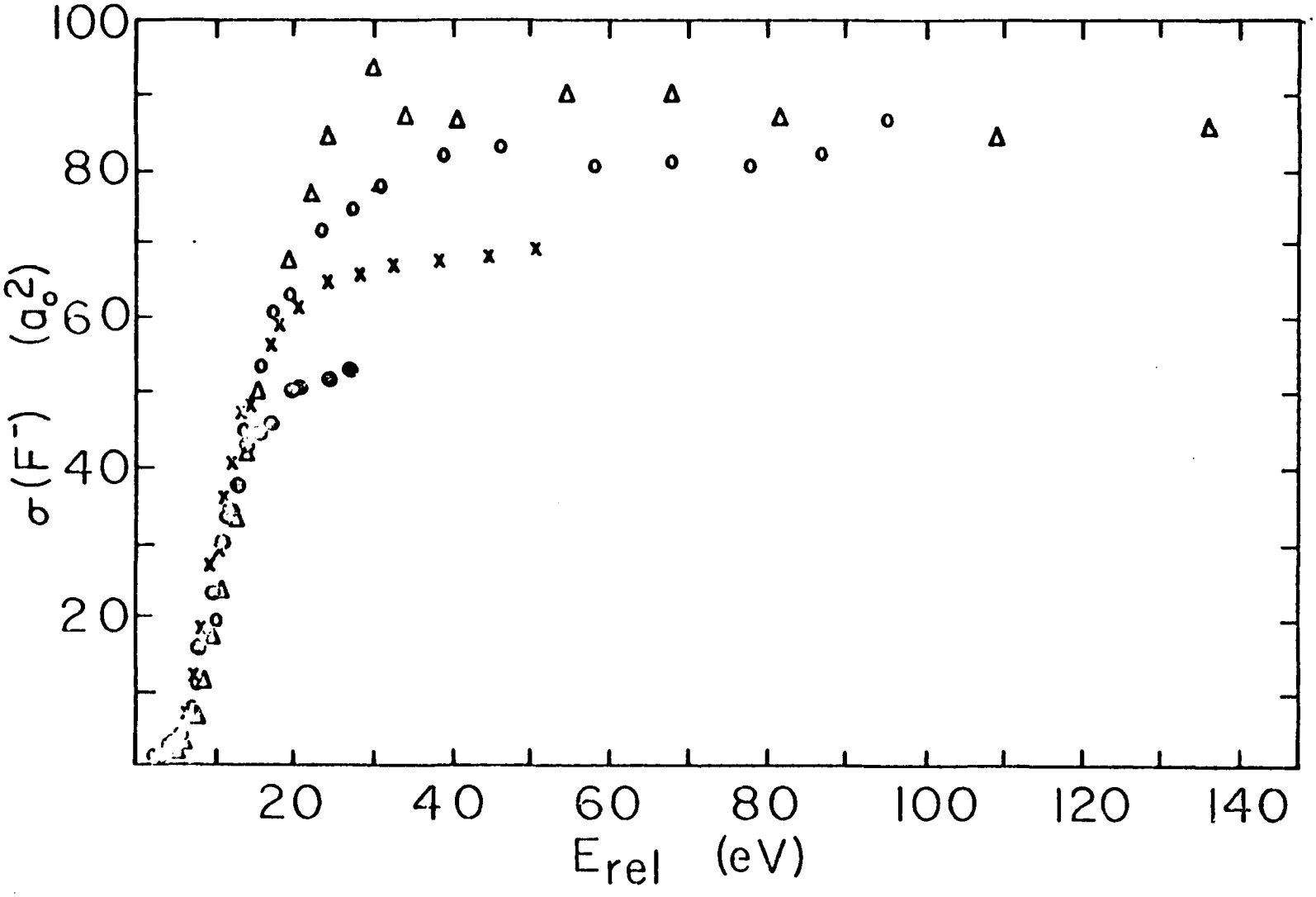
100
80
60
40
20
σ(F⁻) (a₀²)
20
40
60
80
100
120
140
E_rel (eV)

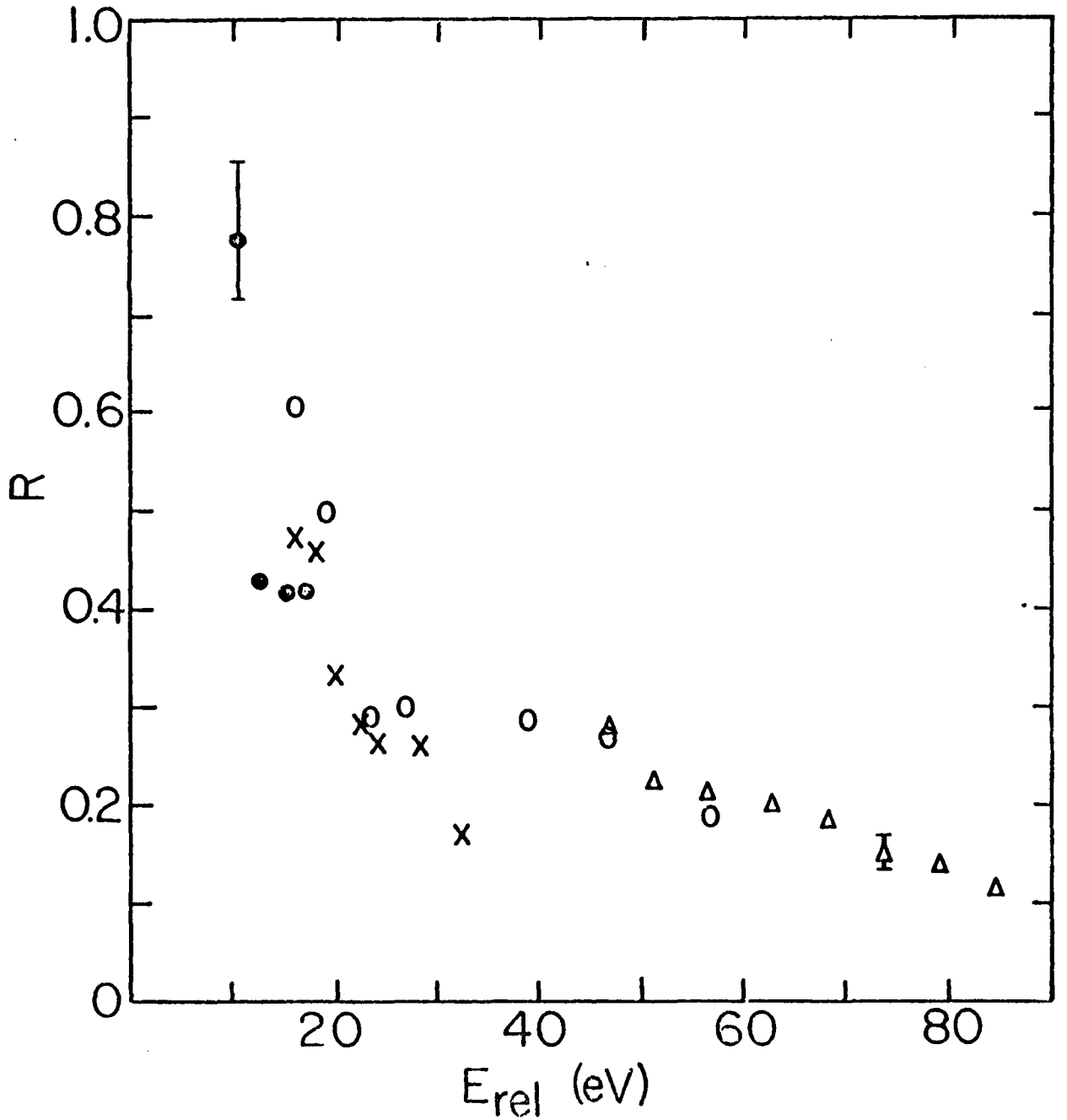

Fig. 6

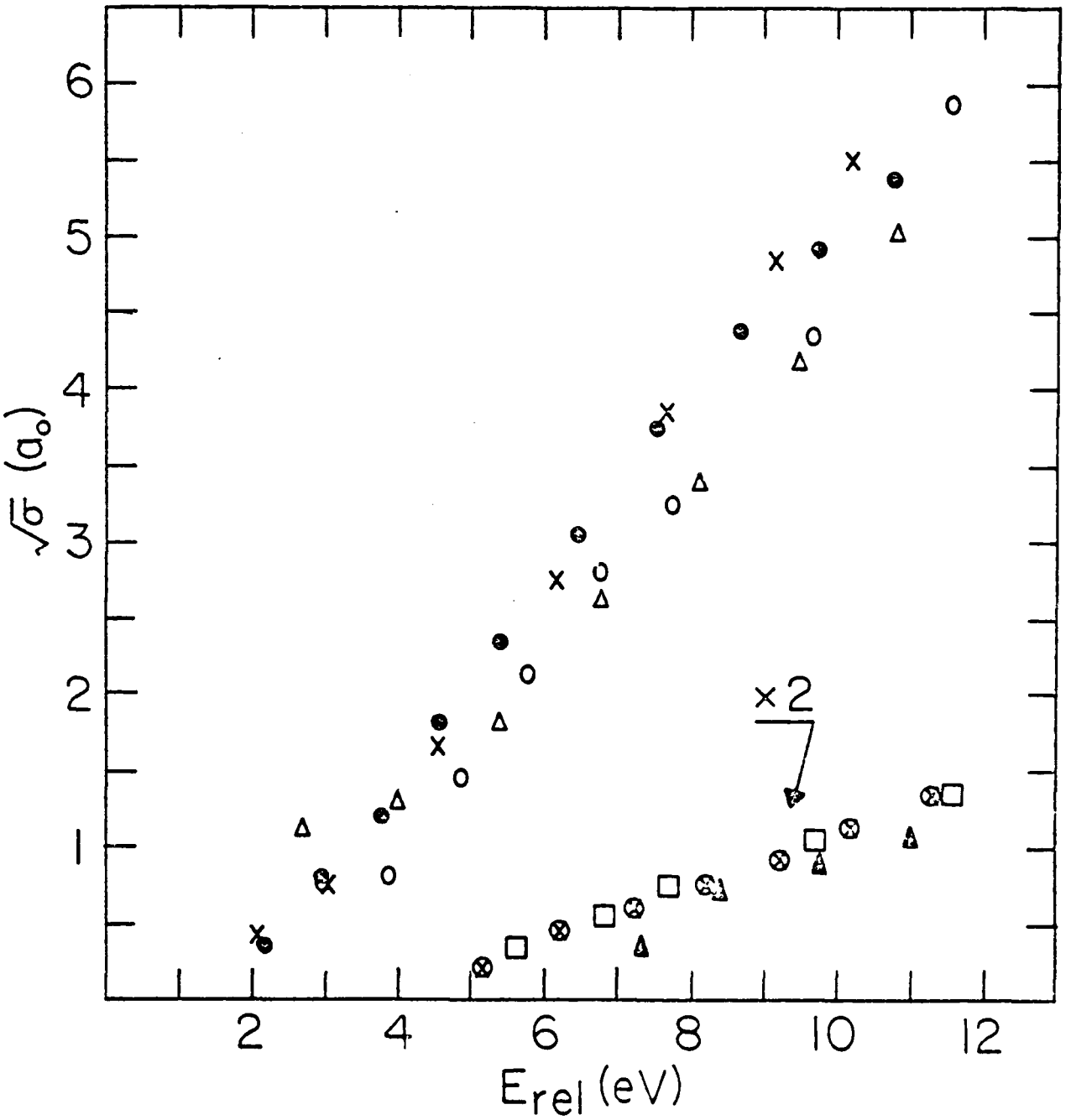

Fig 7

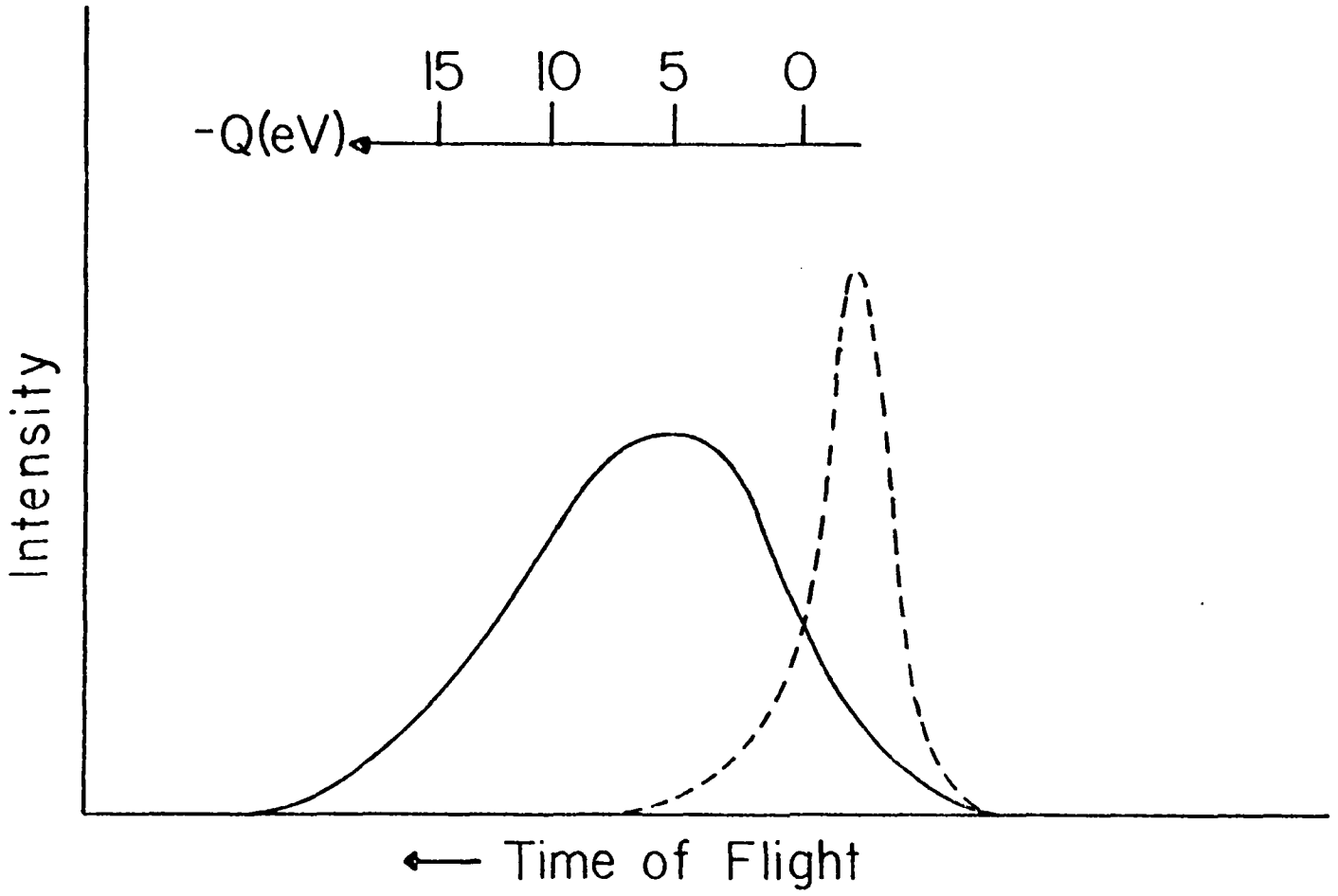
15
10
5
0
-Q(eV)
Intensity
Time of Flight

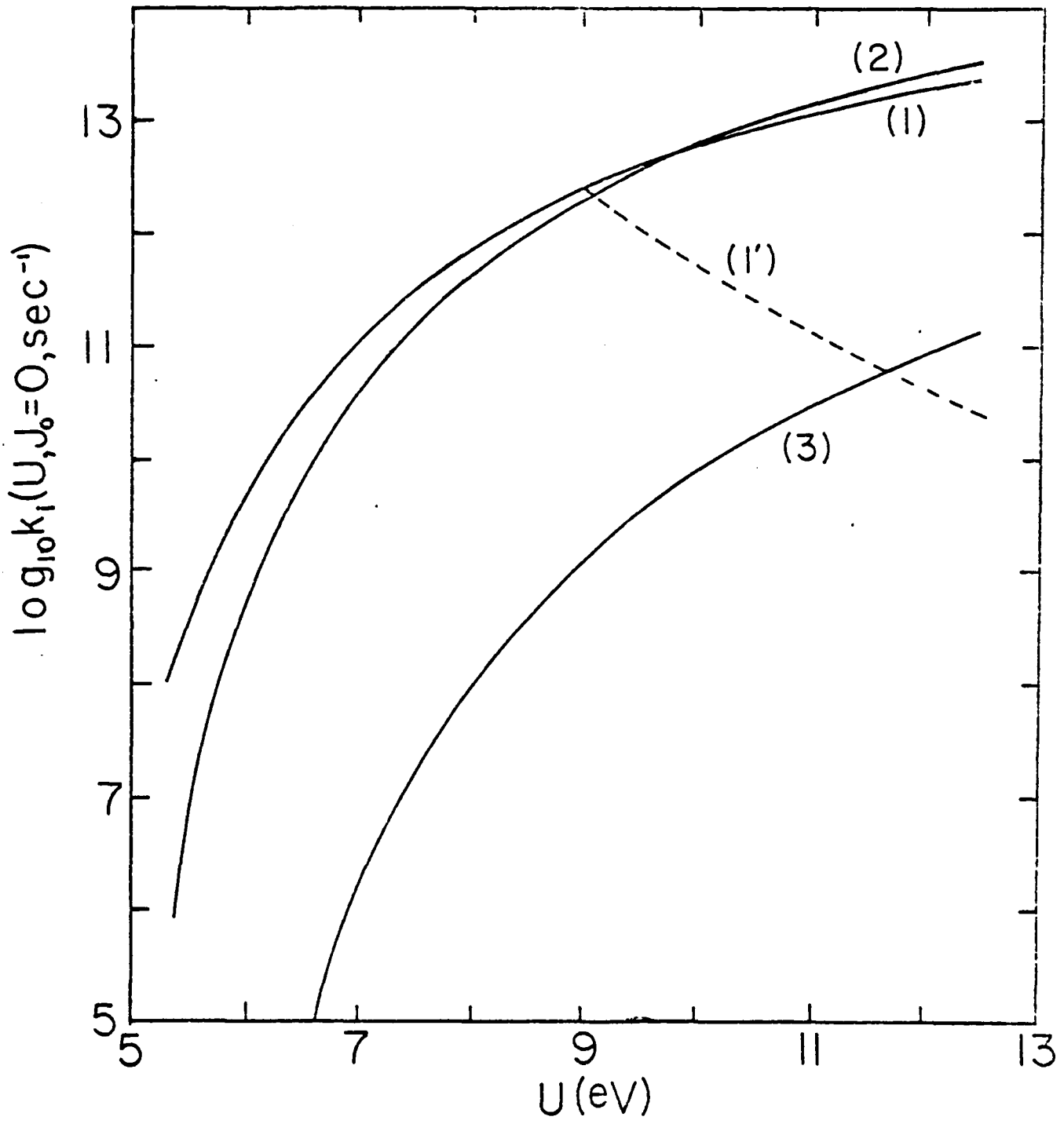

Fig. 4

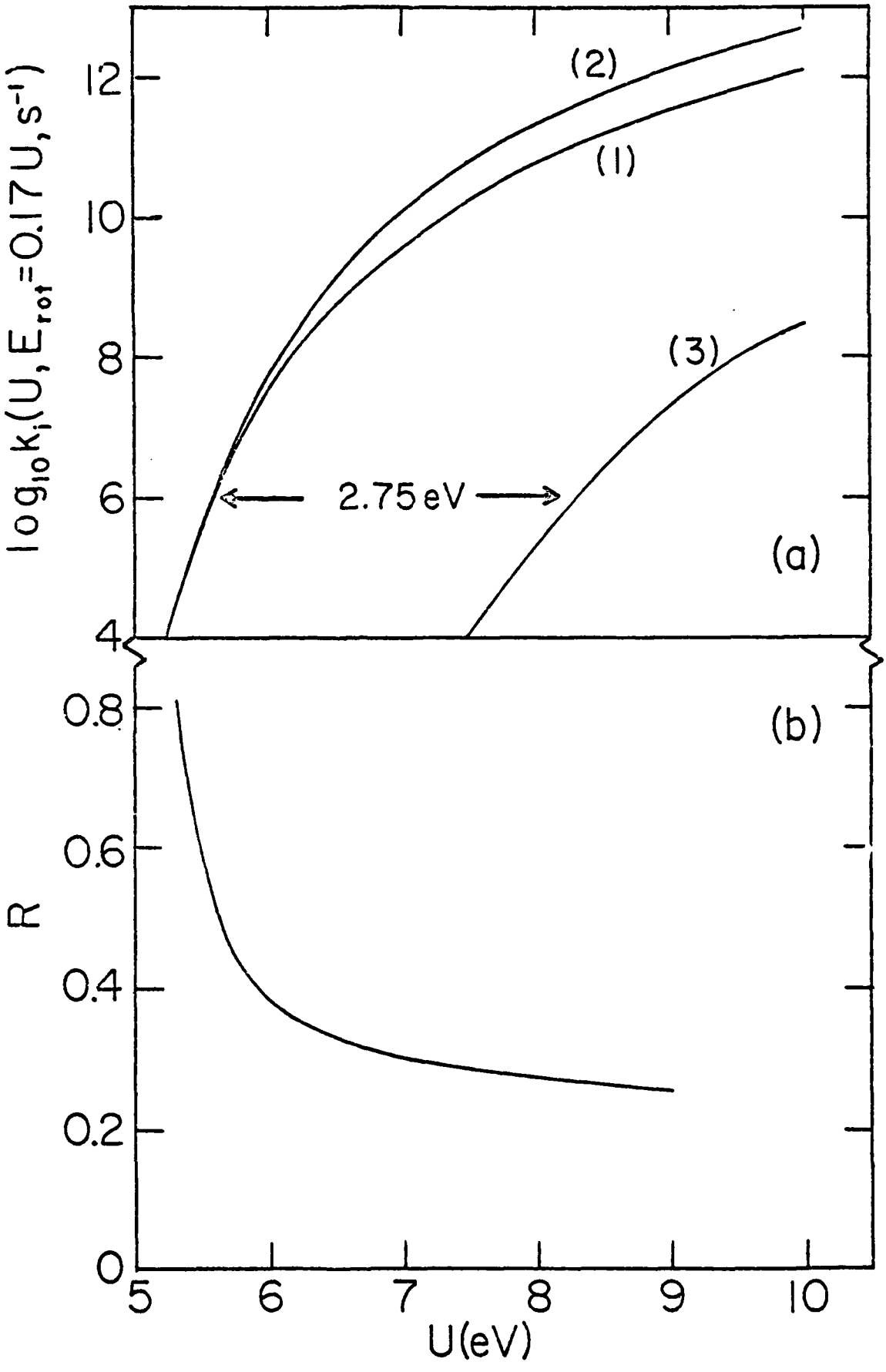
$\log_{10} k_j(U, E_{rot}=0.17U, s^{-1})$
12
10
8
6
4
(2)
(1)
(3)
2.75 eV
(a)
(b)
R
0.8
0.6
0.4
0.2
0
5
6
7
8
9
10
U(eV)


DATE
ILME